Structure of Zirconocene Complexes Relevant for Olefin Catalysis: Infrared Fingerprint of the Zr(C5H5)(2)(OH)(CH3CN)(+) Cation in the Gas Phase

ARTICLE *in* THE JOURNAL OF PHYSICAL CHEMISTRY A · FEBRUARY 2010

Impact Factor: 2.69 · DOI: 10.1021/jp910035w · Source: PubMed

5 AUTHORS, INCLUDING:

Anita Röthke
Physikalisch-Technische Bundesanstalt
19 PUBLICATIONS **301** CITATIONS
SEE PROFILE

Andreas Springer
Freie Universität Berlin
31 PUBLICATIONS **462** CITATIONS
SEE PROFILE

Philippe Maître
Université Paris-Sud 11
140 PUBLICATIONS **3,548** CITATIONS
SEE PROFILE

Structure of Zirconocene Complexes Relevant for Olefin Catalysis: Infrared Fingerprint of the $Zr(C_5H_5)_2(OH)(CH_3CN)^+$ Cation in the Gas Phase

Anita Lagutschenkov,[†] Andreas Springer,[‡] Ulrich Joseph Lorenz,[†,§] Philippe Maitre,[||] and Otto Dopfer*[,†]

Institut für Optik und Atomare Physik, Technische Universität Berlin, Hardenbergstrasse 36, 10623 Berlin, Germany, Institut für Chemie und Biochemie, Freie Universität Berlin, Takustrasse 3, 14195 Berlin, Germany, Laboratoire de Chimie Physique Moléculaire, Ecole Polytechnique Fédérale de Lausanne, EPFL SB ISIC LCPM, Station 6, CH-1015 Lausanne, Switzerland, and Laboratoire de Chimie Physique, Faculté des Sciences, Université Paris-Sud 11, UMR8000 CNRS, Faculté des Sciences, Bât. 350, 91405 Orsay Cedex, France

Received: October 20, 2009; Revised Manuscript Received: December 7, 2009

Cationic zirconocene complexes are active species in Ziegler−Natta catalysis for olefin polymerization. Their structure and metal−ligand bond strength strongly influence their activity. In the present work, the infrared multiphoton dissociation (IRMPD) spectrum of mass selected $Zr(C_5H_5)_2(OH)(CH_3CN)^+$ cations was obtained in the 300−1500 cm^{-1} fingerprint range by coupling a Fourier-transform ion cyclotron resonance (FT-ICR) mass spectrometer equipped with an electrospray ionization (ESI) source and the infrared free electron laser (IR-FEL) at the Centre Laser Infrarouge d'Orsay (CLIO). The experimental efforts are complemented by quantum chemical calculations at the MP2 and B3LYP levels using the 6-311G* basis set. Vibrational assignments of transitions observed in the IRMPD spectra to modes of the Zr−O−H, C_5H_5, and CH_3CN moieties are based on comparison to calculated linear absorption spectra. Both the experimental data and the calculations provide unprecedented information about structure, metal−ligand bonding, charge distribution, and binding energy of the complex.

1. Introduction

Cationic zirconocene complexes with Zr in the oxidation state +4 are relevant intermediates in the catalytic cycle of industrial olefin polymerization, using the so-called Ziegler−Natta process.[1−4] The last twenty years have seen great efforts to develop new single-site polymerization catalysts with higher activity and tailored selectivities. Among them, especially group IV metallocenes have been thoroughly investigated.[5−8] The so-called Arlman−Cossee mechanism is widely accepted to explain their polymerization characteristics.[9−11] In particular, the high electrophilicity of the catalytically active cationic 14 electron species, with $Zr(C_5H_5)_2(CH_3)^+$ representing the prototype, is believed to account for their high reactivity.[1,3,4] At the same time, intermediates of the catalytic cycle were found to be short-lived and thus hard to assay with spectroscopic tools. Furthermore, the inevitably strong interactions with the counteranion and solvent molecules in the condensed phase hamper the description of the intrinsic properties of different catalysts and the analysis of the principles in action during the various steps of the catalytic cycle. Thus, investigations have so far been limited to mass spectrometric studies and the determination of reaction rates in the gas phase.[12−17] In previous spectroscopic work, the frequencies of the CO stretch modes in IR spectra of neutral zirconocene dicarbonyl complexes, with Zr being in the oxidation state +2, have been used as a probe of the electrophilicity of the metal center.[18] However, the relevant catalyst is cationic and, so far, it has not been possible to perform a similar analysis for the ionic system with Zr in the relevant oxidation state +4.

In general, it is experimentally difficult to capture and investigate organometallic reaction intermediates. Mass spectrometry in combination with infrared (IR) spectroscopy has proven to be a challenging but powerful tool to isolate metal−organic complexes isolated in the gas phase and characterize their structure and chemical bonding free from interference with the surrounding environment.[19−24] In particular, the observation of metal−ligand vibrations is desirable; however, spectroscopic data for such modes are extremely scarce.[25,26]

In an effort to understand the individual steps of the catalytic cycle in olefin polymerization using zirconocene based complexes, we aim at the characterization of isolated complexes of the type $Zr(C_5H_5)_2XL^+$ with a variety of functional groups X (e.g., H, OH, CH_3) and ligands L (e.g., CO, CH_3CN, alkenes) by gas-phase IR spectroscopy. Significantly, the resulting IR spectra manifest the first spectroscopic characterization of such cationic Zr complexes isolated in the gas phase, i.e., under conditions without the perturbations of counteranions and solvent molecules. Comparison of the IR spectra with quantum chemical calculations provides detailed insight at the molecular level about structure, energetics, solvation effects, and reactivity of these systems.

Initial results are reported here for $Zr(C_5H_5)_2(OH)(CH_3CN)^+$, i.e., X = OH and L = CH_3CN, an analogue of the industrially relevant $Zr(C_5H_5)_2(CH_3)(olefin)^+$ complexes. The spectroscopic efforts are complemented by quantum chemical calculations at the MP2 and B3LYP levels using the 6-311G* basis set. It is well documented that the fruitful combination of IR spectroscopy and quantum chemical calculations provides direct access

* Corresponding author. E-mail: dopfer@physik.tu-berlin.de. Fax: (+49) 30-31423018.
[†] Technische Universität Berlin.
[‡] Freie Universität Berlin.
[§] Ecole Polytechnique Fédérale de Lausanne.
[||] Université Paris-Sud.

10.1021/jp910035w

to salient features of the potential energy surface of isolated ions and ionic complexes, such as structures, bond strengths, dissociation energies, and charge distributions.[20,27−36]

The complexes of interest were generated by electrospray ionization (ESI). IR spectra of $Zr(C_5H_5)_2(OH)(CH_3CN)^+$ were obtained by means of IR multiphoton dissociation (IRMPD) of mass selected cations in a Fourier-transform ion cyclotron resonance (FT-ICR) mass spectrometer in the 300−1500 cm^{-1} spectral fingerprint range.[37−40] The intense IR radiation required for the dissociation of the strongly bound species was provided by the infrared free electron laser (IR-FEL) at the Centre Laser Infrarouge d'Orsay (CLIO).[41] The IRMPD mechanism and its effects on the appearance of the IR spectrum were discussed previously.[39,42] Essentially, the IRMPD process results in broadening and frequency shifts of the transitions compared to those observed in linear IR absorption spectra.[39,42] The red shifts and widths observed in IRMPD spectra are, however, typically below 30 cm^{-1}, allowing for an assignment of the IRMPD bands by direct comparison with calculated linear IR absorption spectra. This strategy was successfully applied to a large variety of species in the past decade, including organometallic complexes of catalytic interest,[19−21] transition metal−amino acid complexes,[35,43−45] and protonated aromatic molecules.[46−51]

2. Experimental and Theoretical Techniques

The IRMPD spectra of $Zr(C_5H_5)_2(OH)(CH_3CN)^+$ were obtained with the IR-FEL at CLIO coupled to a modified Bruker APEX-Qe FT-ICR mass spectrometer.[21] The FEL is based on a 10−50 MeV electron linear accelerator.[41] At a given electron energy, the photon energy was tuned by adjusting the gap of the undulator, which is placed in the optical cavity. The IR-FEL output consists of 8 μs long macropulses with a repetition rate of 25 Hz. Each macropulse was composed of 500 micropulses, each a few picoseconds long and separated by 16 ns. For a typical IR average power of 500 mW used in the present work, the corresponding micropulse and macropulse energies were 40 μJ and 20 mJ, respectively. The FEL was operated at 40 and 28 MeV for the IRMPD spectra recorded in the 750−1570 and 400−860 cm^{-1} ranges, respectively, with typical step sizes of 2−4 cm^{-1} depending on the laser frequency. The laser wavelength was monitored with a monochromator coupled to a pyroelectric detector array. The IR-FEL spectral width (fwhm) was less than 0.5% of the central wavelength.

The FT-ICR mass spectrometer is equipped with an Apollo II ESI ion source, a quadrupole mass filter, a hexapole accumulation/collision cell, and a 7 T magnet. Initial efforts aimed at the generation of $Zr(C_5H_5)_2CH_3^+$. However, in contrast to a previous report,[15] none of the investigated ionization conditions resulted in the generation of $Zr(C_5H_5)_2(CH_3)^+$ or $Zr(C_5H_5)_2(CH_3)(ligand)^+$ using $Zr(C_5H_5)_2(CH_3)_2$ as a neutral precursor. Therefore, we prepared a 5×10^{-5} molar solution of a salt with $Zr(C_5H_5)_2(CH_3)(CH_3CN)^+$ cations and the bulky tetrakis(pentafluorophenyl)borate$^-$ counteranions dissolved in a dry solution of 99% CH_3CN and 1% $(C_2H_5)_2O$ under an inert gas atmosphere. This solution was sprayed under the following standard ESI conditions: flow rates of 120 μL/h, spray voltages of around 5 kV, drying gas flow of 4 L/s, nebulizer pressure of 1.5 bar, and drying gas temperature of 250 °C. Mass spectra of ions generated by ESI of this solution demonstrated the successful production of Zr bearing ions, such as $Zr(C_5H_5)_2(OH)^+$ and $Zr(C_5H_5)_2(OH)(CH_3CN)^+$. Residual H_2O impurities probably led to the reaction[14,52]

$$Zr(C_5H_5)_2(CH_3)(CH_3CN)^+ + H_2O \rightarrow Zr(C_5H_5)_2(OH)(CH_3CN)^+ + CH_4$$

in quantitative yields on the way of the educt ions from the spray region to the ICR cell, most probably in the hexapole collision cell used to accumulate and thermally relax the ions. The characteristic isotopic pattern of Zr confirmed the proper ion identification and selection (51.5% ^{90}Zr, 11.2% ^{91}Zr, 17.2% ^{92}Zr, 17.4% ^{94}Zr, 2.8% ^{96}Zr). To obtain the IRMPD spectra of $Zr(C_5H_5)_2(OH)(CH_3CN)^+$, ions were first mass-selected in the quadrupole mass filter and then accumulated for 3 s in the collision cell filled with Ar. Subsequently, they were injected into the ICR trap, where they were irradiated for three seconds by the IR-FEL laser beam focused with a 2 m focal mirror.[21]

With the laser tuned to a vibrational transition, the ion absorbed several photons (∼10−20) in a stepwise process until the dissociation threshold was reached.[39,42] By monitoring the intensities of parent (I_{parent}) and resulting fragment ions ($I_{fragment}$) as a function of the laser wavenumber, we obtained the IRMPD spectrum as $R = -\ln(I_{parent}/[I_{parent} + \Sigma I_{fragment}])$. Only the monoisotopic mass (278.0122 u) was considered for the analysis. Despite its multiple photonic nature, the IRMPD spectrum predominantly reflects the absorption of the first IR photon (see ref 39 for a recent review of the IRMPD mechanism). This observation justifies a comparison of the experimental IRMPD spectrum with a calculated linear one-photon IR absorption spectrum.

Quantum chemical calculations were performed at the B3LYP and MP2 levels of theory using the GAUSSIAN03 package.[53] The employed basis set is a combination of the 6-311G* basis[54] for H, C, N, and O and the Stuttgart ECP basis for Zr.[55] For comparison, calculations for structures, energies, and IR spectra were also carried out with the 6-311G(2d,2p) and 6-311G(2df,2pd) basis sets leading to similar results. Hence, only the results obtained with the 6-311G* basis are reported. Stationary points were obtained on a potential energy surface corrected for basis set superposition error.[56] Reported energies were also corrected for harmonic zero point vibrational energies, and vibrational frequencies were scaled by 0.9927 (0.9844) for $\nu < 1800$ cm^{-1} and 0.9659 (9584) for $\nu > 1800$ cm^{-1} at the B3LYP (MP2) level, respectively.[57] Calculations were performed for $Zr(C_5H_5)_2(OH)(CH_3CN)^+$ to evaluate its geometry and IR spectral features as well as its lowest energy fragment ion (observed by IRMPD), $Zr(C_5H_5)_2(OH)^+$, to determine binding energies. The individual subsystems of $Zr(C_5H_5)_2(OH)(CH_3CN)^+$, namely the ligands $C_5H_5^-$, OH^-, and CH_3CN were also considered to evaluate the effects of complex formation on structure, vibrational frequencies, IR intensities and charge distribution. The charge distribution was determined using the natural bond orbital (NBO) analysis.

3. Results and Discussion

Geometry optimization of $Zr(C_5H_5)_2(OH)(CH_3CN)^+$ in its singlet electronic ground state using a variety of different starting geometries yielded a single minimum energy structure depicted in Figure 1. No other stable structure could be located on the potential energy surface. At zeroth order, the complex can be viewed as an intermolecular complex composed of a Zr^{4+} cation, two $C_5H_5^-$ units, OH^-, and a neutral CH_3CN ligand. The NBO analysis at the B3LYP (MP2) level yields charges of +1.62 (+1.92) e on Zr, −0.44 (−0.58) e on OH, −0.19 (−0.26) e on each C_5H_5 moiety, and +0.20 (+0.18) e on CH_3CN, respectively, which strongly deviates from the formal charges of +4,

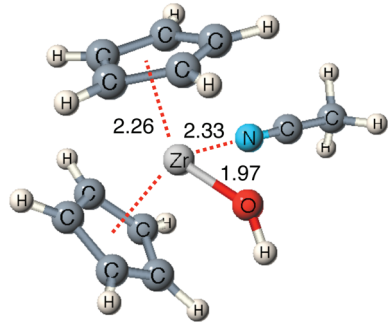

Figure 1. Structure of $Zr(C_5H_5)_2(OH)(CH_3CN)^+$ evaluated at the B3LYP/6-311G* level of theory. Metal−ligand bond distances are given in Å.

−1, −1, and 0 e in the zero-order picture. The NBO charges suggest significant charge transfer and covalent bond contributions, which in turn cause noticeable changes in the geometry and vibrational properties of the individual units upon complex formation. We therefore also consider the properties of these individual subunits to evaluate their changes upon formation of the complex. The relevant structural, energetic, and vibrational parameters are summarized in Table 1. Linear IR absorption spectra of $Zr(C_5H_5)_2(OH)(CH_3CN)^+$ and the corresponding subsystems are compared in Figure 2.

As expected,[3,4,8,18] the global minimum structure of $Zr(C_5H_5)_2(OH)(CH_3CN)^+$ has a distorted, pseudotetrahedral geometry. The two η^5-coordinated cyclopentadienyl ligands are roughly equivalent, with a Zr−ring separation of 2.26 (2.21) Å. The bending angle involving the centers of the C_5H_5 rings and the Zr atom amounts to 131° (130°).

The rather strong Zr−OH bond is characterized by a short separation of 1.97 (1.96) Å, a high covalent bond dissociation energy of 478.8 (416.7) kJ/mol with respect to neutral OH loss,[52] and a bond angle of 141° (143°), whereby the OH group is pointing toward one of the C_5H_5 moieties. The large deviation from linearity is taken as strong evidence for significant covalent and less ionic character of the Zr−OH bond.[58] Similar bond dissociation energies (404 kJ/mol) and bond angles (149.5°) have been recently predicted for the related isovalent $Ti(OH)_3^+$ complex at the B3LYP level.[58] Also, the related neutral $Zr(OH)_4$ molecule converges to a S_4 symmetric structure at the B3LYP level, with an Zr−O−H bond angle of 150° and a Zr−O separation of 1.963 Å,[59] comparable to that in $Zr(C_5H_5)_2(OH)(CH_3CN)^+$, demonstrating the Zr−OH bond character is similar in both species. The Zr−OH bond in $Zr(C_5H_5)_2(OH)(CH_3CN)^+$ is described by a Zr−O stretch frequency of σ_{ZrO} = 657 (665) cm^{-1}, an in-plane bend frequency of β_{ZrOH} = 500 (501) cm^{-1}, and an out-of-plane torsional frequency of γ_{ZrOH} = 357 (318) cm^{-1}, respectively. The theoretical IR spectrum of $Zr(C_5H_5)_2(OH)(CH_3CN)^+$ shown in Figure 2 demonstrates that in particular all three vibrational modes involving the Zr−OH unit (σ_{ZrO}, β_{ZrOH}, γ_{ZrOH}) have large IR oscillator strengths and appear as fingerprints in the 300−700 cm^{-1} range of the spectrum. Moreover, σ_{ZrO} and β_{ZrOH} appear as isolated transitions, demonstrating that IR spectroscopy is a versatile tool to directly probe the Zr−OH interaction.

As expected,[60−64] CH_3CN binds almost linearly to the central Zr atom, with a Zr−N bond distance of 2.33 (2.35) Å and a bond angle of 173° (173°) at the B3LYP (MP2) level. The relatively weak CH_3CN−Zr metal−ligand bond is characterized by an intermolecular stretch frequency of 227 (232) cm^{-1} and

TABLE 1: Relevant Structural, Vibrational, and Energetic Parameters of the $Zr(C_5H_5)_2(OH)(CH_3CN)^+$ Complex and Individual Isolated Ligands Evaluated at the B3LYP and MP2 Levels of Theory[a−c]

ligand/complex	parameter[d]	ligand (B3LYP)	ligand (MP2)	complex (B3LYP)	complex (MP2)
OH^-	R_{OH}/Å	0.9837	0.9717	0.9594	0.9592
	σ_{OH}/cm^{-1}	3266 (460)	3429 (331)	3754 (156)	3743 (213)
CH_3CN	R_{CN}/Å	1.1521	1.1730	1.1498	1.1685
	σ_{CN}/cm^{-1}	2289 (8)	2124 (0)	2304 (119)	2170 (37)
	R_{CC}/Å	1.4569	1.4618	1.4488	1.4554
	σ_{CC}/cm^{-1}	924 (2)	921 (2)	943 (5)	943 (7)
	R_{CH}/Å	1.0919	1.0906	1.0922	1.0912
	σ_{CH}/cm^{-1} (aver)	2992 (5)	3035 (2)	2999 (4)	3035 (4)
	β_{CH_3}/cm^{-1} (aver)	1066 (3)	1069 (3)	1057 (10)	1062 (5)
	β_{CH}/cm^{-1} (aver)	1461 (17)	1473 (19)	1444 (14)	1457(15)
$C_5H_5^-$[e]	R_{CC}/Å (aver)	1.4132	1.4171	1.4182	1.4223
	R_{CH}/Å (aver)	1.0892	1.0901	1.0807	1.0838
	γ_{CH}/cm^{-1} (aver, $\nu_4(a_2'')$)	639 (149)	615 (166)	824 (121)	794 (125)
	γ_{CH}/cm^{-1} (aver, $\nu_8(e_1'')$)	606 (0)	487 (0)	834 (23)	798 (29)
	β_{CH}/cm^{-1} (aver, $\nu_7(e_1')$)	1009 (27)	1011 (28)	1030 (13)	1031 (14)
	σ_{CC}/cm^{-1} (aver, all)	1365 (4)	1378 (3)	1370 (3)	1369 (3)
	σ_{CC}/cm^{-1} (aver, $\nu_6(e_1')$)	1463 (9)	1452 (7)	1467 (4)	1451 (6)
	σ_{CH}/cm^{-1} (aver, all)	3006 (221)	3034 (164)	3129 (0)	3128 (2)
complex	R_{ZrO}/Å			1.9683	1.9634
	σ_{ZrO}/cm^{-1}			657 (46)	665 (55)
	D_0/kJ mol^{-1} (Zr−O bond)			416.7	478.8
	β_{ZrOH}/cm^{-1}			500 (166)	501 (161)
	γ_{ZrOH}/cm^{-1}			357 (147)	318 (133)
	angle Zr−O−H/deg			141.1	142.6
	R_{ZrN}/Å			2.3331	2.3472
	σ_{ZrN}/cm^{-1}			227 (6)	232 (7)
	D_0/kJ mol^{-1} (Zr−N bond)			148.9	158.5

[a] The full data set is listed in Table S1 in Supporting Information. [b] Calculations with the 6-311G* basis for H, O, C, N and the Stuttgart ECP basis for Zr. [c] Frequencies are scaled by 0.9927 (0.9844) for ν < 1800 cm^{-1} and 0.9659 (0.9584) for ν > 1800 cm^{-1} at the B3LYP (MP2) level. IR intensities I are listed in km/mol (in parentheses). [d] The designation "aver" denotes averaged values. [e] Nomenclature for normal modes of $C_5H_5^-$ taken from ref 65.

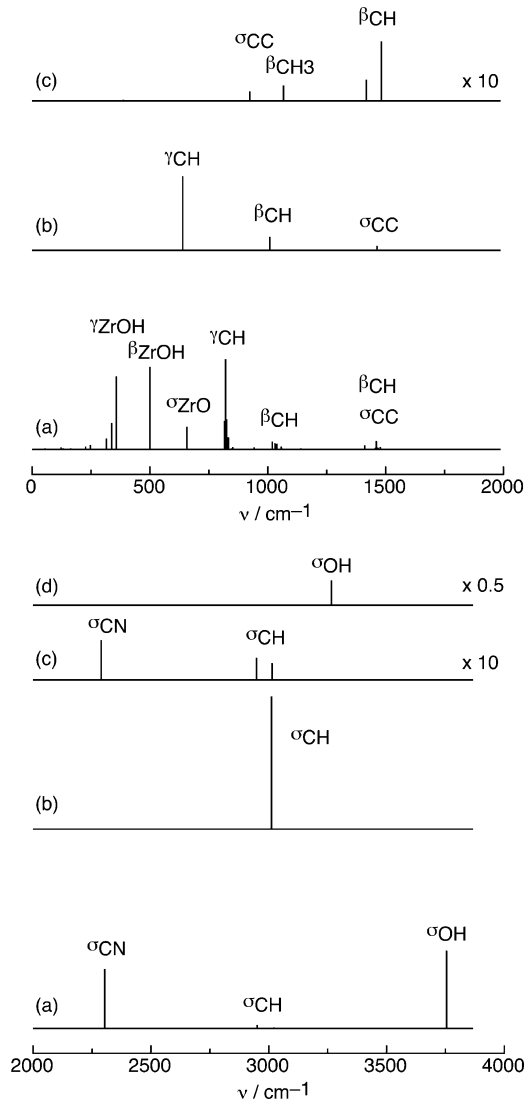

Figure 2. Comparison of linear IR absorption spectra of (a) $Zr(C_5H_5)_2(OH)(CH_3CN)^+$, (b) $C_5H_5^-$, (c) CH_3CN, and (d) OH^- evaluated at the B3LYP/6-311G* level of theory.

a bond dissociation energy of 143.5 (153.5) kJ/mol. The rupture of this bond corresponds to the lowest dissociation channel on the potential energy surface of $Zr(C_5H_5)_2(OH)(CH_3CN)^+$ and is indeed experimentally observed upon IR activation.

After discussing the intermolecular metal−ligand bond parameters, we now turn our attention toward the intramolecular properties of the individual ligand subunits in the complex using the B3LYP data (Table 1). For both the CH_3CN and the C_5H_5 units, complexation completely removes the symmetry from C_{3v} and D_{5h}, respectively, implying that degenerate vibrations in the monomers are split in the complex. In the following (and in Table 1), we mainly consider the corresponding average values for bond distances, vibrational frequencies and IR intensities, denoted by superscript "aver", to evaluate qualitative trends in structural and vibrational properties upon complex formation. Individual data are provided in Table S1 in Supporting Information.

The OH bond in $Zr(C_5H_5)_2(OH)(CH_3CN)^+$ is significantly shorter than that in bare OH^- (0.9594 vs 0.9837 Å), giving rise to a large blue shift in the OH stretch frequency, σ_{OH} (3754 vs 3266 cm^{-1}). This observation is consistent with the significant charge donation from OH^- to the Zr cation, leaving only −0.44 e on the OH group. For the related neutral $Zr(OH)_4$ complex, the OH stretch frequencies were indeed identified at around 3780 cm^{-1} in IR spectra recorded in an argon matrix,[59] indicative of substantial charge transfer from the four equivalent OH^- ligands to the central Zr^{4+} ion also in this molecule.

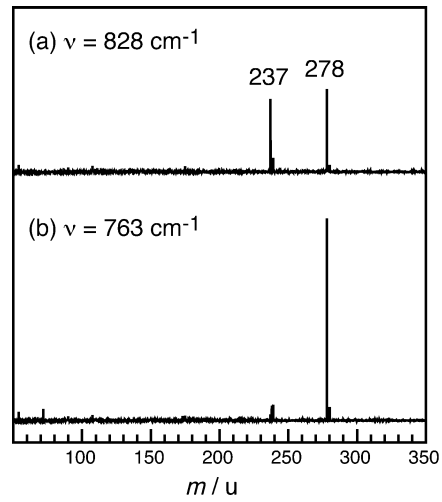

Figure 3. Mass spectra obtained by isolating $Zr(C_5H_5)_2(OH)(CH_3CN)^+$ with $m = 278$ u in the ICR cell and subsequent FEL irradiation at the vibrational resonance at $\nu = 828$ cm^{-1} (a) and off resonance at $\nu = 763$ cm^{-1} (b). $Zr(C_5H_5)_2(OH)^+$ with $m = 237$ u corresponding to the elimination of CH_3CN is the only fragment channel observed upon IR activation.

The complexation-induced changes in the CH_3CN properties are much smaller,[60−64] consistent with the modest positive charge of 0.2 e for this ligand in the complex. The CN and CC bonds slightly contract (1.521 vs 1.1498 Å, 1.4569 vs 1.4488 Å), leading to small increases in the corresponding stretch frequencies (σ_{CN} = 2289 vs 2304 cm^{-1}, σ_{CC} = 924 vs 943 cm^{-1}). In contrast, the CH bond lengths (1.0919 vs 1.0922 Å) and averaged stretch frequencies (σ_{CH}^{aver} = 2992 vs 2999 cm^{-1}) are similar. Simultaneously, both the N−C−CH_3 and C−C−H bend frequencies decrease ($\beta_{CH_3}^{aver}$ = 1066 vs 1075 cm^{-1}, β_{CH}^{aver} = 1461 vs 1444 cm^{-1}).

As the charge on each C_5H_5 unit is only −0.19 e, a larger complexation effect is observed for the $C_5H_5^-$ ligands. The CH bonds contract from 1.0892 to 1.0815 Å, causing a significant increase in the CH stretch frequency σ_{CH}^{aver} of 123 cm^{-1} from 3006 to 3129 cm^{-1}. Significantly, the large IR intensity of the IR allowed CH stretch mode ($I = 533$ km/mol for $\nu_5(e_1')$) nearly vanishes upon complex formation ($I < 3$ km/mol), so that they are invisible in the calculated spectrum in Figure 2. The CC bond length is roughly the same (1.4132 vs 1.4182 Å), leading to similar CC stretch frequencies (σ_{CC}^{aver} = 1365 vs 1370 cm^{-1}). The in-plane CH bend frequencies of the C_5H_5 units are also relatively unaffected (β_{CH}^{aver} = 843, 1009, 1052, 1266 vs 855, 1030, 1082, 1290 cm^{-1}), whereas all out-of-plane CH bend modes drastically increase in frequency (γ_{CH}^{aver} = 553, 606, 639, 717 vs 599, 824, 833, 917 cm^{-1}). It is not clear whether this effect is due to a stiffer out-of-plane CH bend force field of the C_5H_5 unit itself or due to the additional retarding force induced by the C_5H_5−Zr interaction. The latter argument has been used to rationalize blue shifts of similar magnitude in out-of-plane CH bending frequencies of related complexes of benzene with metal cations.[20,22−24]

Figure 3 shows mass spectra obtained by isolating $Zr(C_5H_5)_2(OH)(CH_3CN)^+$ with $m = 278$ u in the ICR cell with subsequent FEL irradiation at the strong vibrational resonance at $\nu = 828$ cm^{-1} (a) and off resonance at $\nu = 763$ cm^{-1} (b). $Zr(C_5H_5)_2(OH)^+$ with $m = 237$ u corresponding to the elimina-

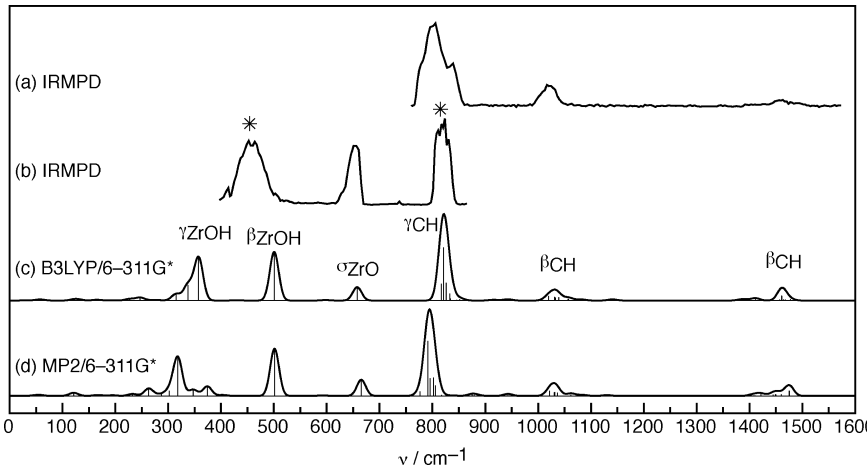

Figure 4. IRMPD spectra of $Zr(C_5H_5)_2(OH)(CH_3CN)^+$ monitored in the $Zr(C_5H_5)_2(OH)^+$ fragment channel and recorded in two different frequency ranges, 760−1570 cm^{-1} (a) and 400−860 cm^{-1} (b), are compared to linear IR absorption spectra calculated at the B3LYP/6-311G* (c) and MP2/6-311G* (d) levels of theory using a convolution width of 20 cm^{-1} (fwhm). Transitions marked by asterisks are saturated. The IR spectra in the low-frequency range show bending and stretching modes of the Zr−OH unit, whereas the bands in the high-frequency range are attributed to vibrations of the C_5H_5 and CH_3CN moieties.

TABLE 2: Experimental Band Centers, Widths (in Parentheses) and Major Vibrational Assignments of the Transitions Observed in the IRMPD Spectra of $Zr(C_5H_5)_2(OH)(CH_3CN)^+$ Compared to Calculated Values[a]

ν_{exp}/cm^{-1}	ν_{calc}/cm^{-1} (B3LYP)[a]	ν_{calc}/cm^{-1} (MP2)[a]	assignment
455 (50)[c]	500 (166)	501 (161)	β_{ZrOH} ZrOH in-plane bend
650 (25)[c]	657 (46)	665 (55)	σ_{ZrO} ZrO stretch
820 (35)[c]	817 (58)	777 (16)	γ_{CH} out-of-plane CH bend (C_5H_5)
800 (50) [d]	821 (181)	791 (187)	
840 (25)[d]	833 (24)	795 (60)	
		801 (63)	
		805 (36)	
1020 (40)[d]	1020 (16)	1022 (18)	β_{CH} in-plane CH bend (C_5H_5)
	1030 (13)	1031 (12)	
	1032 (11)	1032 (13)	
	1038 (12)	1037 (11)	
1435 (30)[d]	1460 (17)	1475 (18)	β_{CH} CH bend (CH_3CN)
1465 (25)[d]	1461 (16)	1477 (18)	*b*

[a] Frequencies are scaled by 0.9927 (0.9844) at the B3LYP (MP2) level. IR intensities *I* are listed in km/mol (in parentheses). Only vibrations with $I > 10$ km/mol are listed. Calculations are carried out with the 6-311G* basis for H, O, C, N and the Stuttgart ECP basis for Zr. [b] In-plane CH bends of C_5H_5 are in the same frequency range but slightly less IR active. [c] From 400 to 860 cm^{-1} scan (Figure 4b). [d] From 760 to 1570 cm^{-1} scan (Figure 4a).

tion of CH_3CN is the only fragment channel observed upon IR activation. The depletion at the resonance is of the order of 50%, demonstrating efficient IRMPD. The calculated binding energy of 144 kJ/mol corresponds to 15 photons with $\nu = 828$ cm^{-1}.

Figure 4 compares the IRMPD spectra of $Zr(C_5H_5)_2(OH)(CH_3CN)^+$ recorded in the 750−1570 and 400−860 cm^{-1} ranges with linear IR absorption spectra calculated at the B3LYP and MP2 levels using a convolution width of 20 cm^{-1} (fwhm). The centers and widths of the experimental transitions observed are listed in Table 2, along with the major vibrational assignments. In general, both calculated spectra are in good agreement with each other and with the experimental spectrum, readily facilitating the assignment of the observed spectrum. The IRMPD line width intrinsically depends on the finite laser bandwidth of 0.5% (corresponding to $\Delta\nu = 2.5-7.5$ cm^{-1} for $\nu = 500-1500$ cm^{-1}), and spectral broadening arising from the multiphotonic character of the IRMPD process.[21,39,42] Using the same experimental conditions, when ions are thermally cooled through multiple collisions with argon in the hexapole accumulation ion-trap at room temperature, IRMPD bands with a width of the order of 15 cm^{-1} could be observed.[21] In the present case, IRMPD bands have widths between 25 and 50 cm^{-1} depending on congestion due to overlapping transitions.

The Zr−O stretch mode is observed at a frequency of $\sigma_{ZrO} = 650$ cm^{-1}, which compares favorably with the computed values of 657 (B3LYP) and 665 (MP2) cm^{-1}. The band at 455 cm^{-1} is assigned to the in-plane Zr−O−H bend calculated at $\beta_{ZrOH} = 500$ and 501 cm^{-1}. Both modes are relatively isolated from other vibrations so that the observed bands can be assigned to single vibrational transitions, providing useful information on the Zr−OH interaction. The experimental σ_{ZrO} frequency of $Zr(C_5H_5)_2(OH)(CH_3CN)^+$ of 650 cm^{-1} is close to the corresponding averaged value of the related tetrahedral $Zr(OH)_4$ molecule measured in solid argon, $\sigma_{ZrO} = 681$ cm^{-1},[59] indicating that the Zr−OH bond strengths in both closed-shell Zr^{IV} complexes are quite similar.

The band observed around 820 cm^{-1} in the IRMPD spectra is safely assigned to the various overlapping out-of-plane C−H bend modes of the C_5H_5 moieties (γ_{CH}), which are calculated to occur in the 815−845 (B3LYP) and 775−820 (MP2) cm^{-1} ranges. In the $C_5H_5^-$ monomer, the corresponding IR active mode is calculated to be of much lower frequency, $\nu_4(a_2'') =$ 639 (B3LYP) and 615 (MP2) cm^{-1}, implying a substantial blue shift of around 180 cm^{-1} upon complex formation (~30%). Unfortunately, the frequencies of isolated $C_5H_5^-$ are not known experimentally, preventing an evaluation of the experimental frequency shift. Only vibrational frequencies of $C_5H_5^-M^+$ salt solutions with various metal ions M^+ are available.[65,66] They, however, scatter largely, again emphasizing the significant impact of metal ions on this particular $C_5H_5^-$ vibrational frequency. As for complexes of benzene with metal cations,[20,22−24] it is likely that this out-of-plane CH bending mode is very sensitive to the binding of $C_5H_5^-$ to the metal, and the corresponding frequency could be an interesting probe of the binding strength of $Zr(C_5H_5)_2(CH_3)^+$ to various ligands.

The band observed at 1020 cm^{-1} in the IRMPD spectrum is attributed to in-plane bend C−H bend modes of the C_5H_5 moieties (β_{CH}), which are calculated to occur in the 1020−1040 range (B3LYP and MP2). The corresponding $C_5H_5^-$ monomer mode is the doubly degenerate, IR allowed $\nu_7(e_1')$ vibration, which splits into its components in the complex. The calculations predict a blue shift of 20 cm^{-1} upon complexation. The

degenerate β_{CH_3} bend of CH_3CN is calculated to occur at a slightly higher frequency (1052−1072 cm^{-1}) and a 5 times weaker intensity than the ν_7 modes of $C_5H_5^-$, indicating that the former modes are probably not contributing to the experimental 1020 cm^{-1} band.

The assignments of the weak bands observed at 1435 and 1465 cm^{-1} in the IRMPD spectrum are less certain. The calculations predict the three C−H bend vibrations of CH_3CN at 1411, 1460, and 1461 (B3LYP) cm^{-1} and 1421, 1475, and 1476 (MP2) cm^{-1} with a total IR intensity of 42 and 44 km/mol. As expected, the shifts from the corresponding frequencies of bare CH_3CN (estimated at ∼1390 and ∼1450)[67] induced by metal complexation are modest due to the weak Zr−$NCCH_3$ interaction. The C−C stretch modes corresponding to the IR active $\nu_6(e_1')$ modes of $C_5H_5^-$ are also expected in this spectral range, with calculated averaged frequencies of 1466 and 1451 cm^{-1}. However, the lower total IR intensity of 14 and 22 km/mol suggest that their contribution to the experimental 1465 cm^{-1} band is minor.

4. Conclusions

The structure and bonding of a cationic zirconocene complex, namely $Zr(C_5H_5)_2(OH)(CH_3CN)^+$, has been investigated by quantum chemical calculations and IRMPD spectroscopy of mass-selected species in the 300−1500 cm^{-1} fingerprint range. Significantly, the analysis of the vibrational frequencies provides a first impression about the Zr−OH metal−ligand bond strength. These preliminary experiments demonstrate that this combined strategy of ESI mass spectrometry, gas-phase infrared spectroscopy and quantum chemistry can yield very valuable results on intermediates in the catalytic cycle of alkene polymerization using Zr catalysts. Future efforts include recording IR spectra of $Zr(C_5H_5)_2(OH)(CH_3CN)^+$ in the OH and CN stretch range to directly probe the effects of complex formation on the charge transfer from the OH group to the central Zr ion as well as the strength of the CH_3CN−Zr ligand−metal bond. In particular, the σ_{CN} stretch frequency of the C≡N triple bond can be employed as a sensitive probe for the electrophilicity of the metal center,[60−64,68] as it depends strongly on the modification of the electronic structure through the C_5H_5 ligands in a number of different catalysts. In addition, the frequency of the out-of-plane CH bending mode of the $C_5H_5^-$ ligands can also be an interesting probe of the binding strength of $Zr(C_5H_5)_2(CH_3)^+$ to various ligands.

Furthermore, also complexes of the type $Zr(C_5H_5)_2(CH_3)(C_nH_m)^+$ with unsaturated hydrocarbon molecules are interesting targets to probe intermediates in olefin polymerization with spectroscopic tools. As a long-term goal of these efforts, new light will be shed on the mechanism and individual steps of the catalytic cycle and new insight will be gained into the principles that govern the reactivity and selectivity of the catalytically active species. Thus, we aim to contribute to the knowledge necessary for the rational design of new catalysts.

Acknowledgment. This study was supported by the *Deutsche Forschungsgemeinschaft* (DO 729/2), the *Fonds der Chemischen Industrie*, and the European Union (EPITOPES 15637, subproject IC 018-07 entitled *IRMPD spectroscopy of intermediates in the catalytic cycle of alkene polymerization*). We thank the groups of H. Braunschweig (University of Würzburg) and N. Mezailles (Ecole Polytechnique Paris) for their support in sample preparation. We also appreciate the support by the CLIO team (J. M. Ortega, C. Six, G. Perilhous, J. P. Berthet).

Supporting Information Available: Table S1 of structural, vibrational, and energetic parameters of the $Zr(C_5H_5)_2(OH)(CH_3CN)^+$ complex and individual isolated ligands evaluated at the B3LYP and MP2 levels of theory. Full list of authors of ref 53. This material is available free of charge via the Internet at http://pubs.acs.org.

References and Notes

(1) Elschenbroich, C. *Organometallics*; 3rd ed.; Wiley: Weinheim, 2006.
(2) Corradini, P.; Guerra, G.; Cavallo, L. *Acc. Chem. Res.* **2004**, *37*, 231–241.
(3) Brintzinger, H. H.; Fischer, D.; Mulhaupt, R.; Rieger, B.; Waymouth, R. M. *Angew. Chem. Int. Ed.* **1995**, *34*, 1143.
(4) Special issue of *Chemical Reviews* devoted to the topic "Frontiers in Metal-Catalyzed Polymerization" (issue 4, April 2000).
(5) Hlatky, G. G. *Chem. Rev.* **2000**, *100*, 1347.
(6) Alt, H. G.; Koppl, A. *Chem. Rev.* **2000**, *100*, 1205.
(7) Coates, G. W. *Chem. Rev.* **2000**, *100*, 1223–1252.
(8) Resconi, L.; Cavallo, L.; Fait, A.; Piemontesi, F. *Chem. Rev.* **2000**, *100*, 1253.
(9) Cossee, P. *J. Catal.* **1964**, *3*, 80.
(10) Arlman, E. J. *J. Catal.* **1964**, *3*, 89.
(11) Arlman, E. J.; Cossee, P. *J. Catal.* **1964**, *3*, 99.
(12) Feichtinger, D.; Plattner, D. A.; Chen, P. *J. Am. Chem. Soc.* **1998**, *120*, 7125.
(13) Chen, P. *Angew. Chem. Int. Ed.* **2003**, *42*, 2832–2847.
(14) Richardson, D. E.; Alameddin, N. G.; Ryan, M. F.; Hayes, T.; Eyler, J. R.; Siedle, A. R. *J. Am. Chem. Soc.* **1996**, *118*, 11244.
(15) Codato, S.; Carta, G.; Rossetto, G.; Zanella, P.; Gioacchini, A. M.; Traldi, P. *Rapid Commun. Mass Spectrom.* **1998**, *12*, 1981.
(16) Plattner, D. A. *Int. J. Mass Spectrom.* **2001**, *207*, 125.
(17) di Lena, F.; Chen, P. *Helv. Chim. Acta* **2009**, *92*, 890.
(18) Zachmanoglou, C. E.; Docrat, A.; Bridgewater, B. M.; Parkin, G.; Brandow, C. G.; Bercaw, J. E.; Jardine, C. N.; Lyall, M.; Green, J. C.; Keister, J. B. *J. Am. Chem. Soc.* **2002**, *124*, 9525.
(19) Simon, A.; Jones, W.; Ortega, J. M.; Boissel, P.; Lemaire, J.; Maitre, P. *J. Am. Chem. Soc.* **2004**, *126*, 11666.
(20) MacAleese, L.; Maitre, P. *Mass Spectrom. Rev.* **2007**, *26*, 583.
(21) Bakker, J. M.; Besson, T.; Lemaire, J.; Scuderi, D.; Maitre, P. *J. Phys. Chem. A* **2007**, *111*, 13415.
(22) Duncan, M. A. *Int. J. Mass Spectrom.* **2008**, *272*, 99.
(23) Jaeger, T. D.; van Heijnsbergen, D.; Klippenstein, S. J.; von Helden, G.; Meijer, G.; Duncan, M. A. *J. Am. Chem. Soc.* **2004**, *126*, 10981.
(24) van Heijnsbergen, D.; von Helden, G.; Meijer, G.; Maitre, P.; Duncan, M. A. *J. Am. Chem. Soc.* **2002**, *124*, 1562.
(25) Swart, I.; de Groot, F. M. F.; Weckhuysen, B. M.; Rayner, D. M.; Meijer, G.; Fielicke, A. *J. Am. Chem. Soc.* **2008**, *13*, 2126.
(26) Fielicke, A.; von Helden, G.; Meijer, G.; Pedersen, D. B.; Simard, B.; Rayner, D. M. *J. Am. Chem. Soc.* **2005**, *127*, 8416.
(27) Roscioli, J. R.; McCunn, L. R.; Johnson, M. A. *Science* **2007**, *316*, 249.
(28) Duncan, M. A. *Int. Rev. Phys. Chem.* **2003**, *22*, 407.
(29) Duncan, M. A. *Int. J. Mass Spectrom.* **2000**, *200*, 545.
(30) Dopfer, O. *Z. Phys. Chem.* **2005**, *219*, 125.
(31) Dopfer, O. *Int. Rev. Phys. Chem.* **2003**, *22*, 437.
(32) Dopfer, O. *J. Phys. Org. Chem.* **2006**, *19*, 540.
(33) Bieske, E. J.; Dopfer, O. *Chem. Rev.* **2000**, *100*, 3963.
(34) Fridgen, T. D. *Mass Spectrom. Rev.* **2009**, *28*, 586.
(35) Polfer, N. C.; Oomens, J. *Mass Spectrom. Rev.* **2009**, *28*, 468.
(36) Eyler, J. R. *Mass Spectrom. Rev.* **2009**, *28*, 448.
(37) Lemaire, J.; Boissel, P.; Heninger, M.; Mauclaire, G.; Bellec, G.; Mestdagh, H.; Simon, A.; Le Caer, S.; Ortega, J. M.; Glotin, F.; Maitre, P. *Phys. Rev. Lett.* **2002**, *89*, 273002.
(38) Maitre, P.; Le Caer, S.; Simon, A.; Jones, W.; Lemaire, J.; Mestdagh, H.; Heninger, M.; Mauclaire, G.; Boissel, P.; Prazeres, R.; Glotin, F.; Ortega, J. M. *Nucl. Instrum. Methods, Sect. A* **2003**, *507*, 541.
(39) Oomens, J.; Sartakov, B. G.; Meijer, G.; von Helden, G. *Int. J. Mass Spectrom.* **2006**, *254*, 1.
(40) Valle, J. J.; Eyler, J. R.; Oomens, J.; Moore, D. T.; van der Meer, A. F. G.; von Helden, G.; Meijer, G.; Hendrickson, C. L.; Marshall, A. G.; Blakney, G. T. *Rev. Sci. Instrum.* **2005**, *76*, 023103.
(41) Prazeres, R.; Glotin, F.; Insa, C.; Jaroszynski, D. A.; Ortega, J. M. *Eur. Phys. J. D* **1998**, *3*, 87.
(42) Oomens, J.; Tielens, A. G. G. M.; Sartakov, B. G.; von Helden, G.; Meijer, G. *Astrophys. J.* **2003**, *591*, 968.
(43) Polfer, N. C.; Oomens, J.; Moore, D. T.; von Helden, G.; Meijer, G.; Dunbar, R. C. *J. Am. Chem. Soc.* **2006**, *128*, 517.
(44) Oomens, J.; Moore, D. T.; von Helden, G.; Meijer, G.; Dunbar, R. C. *J. Am. Chem. Soc.* **2004**, *126*, 724–725.

(45) Moore, D. T.; Oomens, J.; Eyler, J. R.; von Helden, G.; Meijer, G.; Dunbar, R. C. *J. Am. Chem. Soc.* **2005**, *127*, 7243.
(46) Dopfer, O.; Solcà, N.; Lemaire, J.; Maitre, P.; Crestoni, M. E.; Fornarini, S. *J. Phys. Chem. A* **2005**, *109*, 7881.
(47) Chiavarino, B.; Crestoni, M. E.; Fornarini, S.; Dopfer, O.; Lemaire, J.; Maitre, P. *J. Phys. Chem. A* **2006**, *110*, 9352.
(48) Lorenz, U. J.; Lemaire, J.; Maitre, P.; Crestoni, M. E.; Fornarini, S.; Dopfer, O. *Int. J. Mass Spectrom.* **2007**, *267*, 43.
(49) Dopfer, O.; Lemaire, J.; Maitre, P.; Crestoni, M. E.; Fornarini, S. *Int. J. Mass Spectrom.* **2006**, *249*−*250*, 149.
(50) Lorenz, U. J.; Solca, N.; Lemaire, J.; Maitre, P.; Dopfer, O. *Angew. Chem., Int. Ed.* **2007**, *46*, 6714.
(51) Oomens, J.; von Helden, G.; Meijer, G. *Int. J. Mass Spectrom.* **2006**, *249*−*250*, 199.
(52) Richardson, D. E.; Lang, G. H. L.; Crestoni, E.; Ryan, M. F.; Eyler, J. R. *Int. J. Mass Spectrom.* **2001**, *204*, 255.
(53) Frisch, M. J. Gaussian 03, revision C.02; Gaussian, Inc: Pittsburgh PA, 2004.
(54) Krishnan, R.; Binkley, J. S.; Seeger, R.; Pople, J. A. *J. Chem. Phys.* **1980**, *72*, 650.
(55) Andrae, D.; Haussermann, U.; Dolg, M.; Stoll, H.; Preuss, H. *Theor. Chim. Acta* **1990**, *77*, 123.
(56) Boys, S. F.; Bernardi, F. *Mol. Phys.* **1970**, *19*, 553.
(57) Halls, M. D.; Velkovski, J.; Schlegel, H. B. *Theor. Chem. Acc.* **2001**, *105*, 413.
(58) Ricca, A.; Bauschlicher, C. W. *J. Phys. Chem. A* **1997**, *101*, 8949.
(59) Wang, X. F.; Andrews, L. *J. Phys. Chem. A* **2005**, *109*, 10689.
(60) Brackemeyer, T.; Erker, G.; Frohlich, R. *Organometallics* **1997**, *16*, 531.
(61) Brackemeyer, T.; Erker, G.; Frohlich, R.; Prigge, J.; Peuchert, U. *Chem. Ber.-Recl.* **1997**, *130*, 899.
(62) Hijazi, A. K.; Al Hmaideen, A.; Syukri, S.; Radhakrishnan, N.; Herdtweck, E.; Voit, B.; Kuhn, F. E. *Eur. J. Inorg. Chem.* **2008**, 2892.
(63) Buschmann, W. E.; Miller, J. S. *Chem.—Eur. J.* **1998**, *4*, 1731.
(64) Michelin, R. A.; Mozzon, M.; Bertani, R. *Coord. Chem. Rev.* **1996**, *147*, 299.
(65) Bencze, E.; Mink, J.; Nemeth, C.; Herrmann, W. A.; Lokshin, B. V.; Kuhn, F. E. *J. Organomet. Chem.* **2002**, *642*, 246.
(66) Nakamoto, K. *Infrared and Raman Spectra of Inorganic and Coordination Compounds*; 5th ed.; Wiley: New York, 1997; Part B.
(67) Begue, D.; Carbonniere, P.; Pouchan, C. *J. Phys. Chem. A* **2005**, *109*, 4611.
(68) Reinhard, B. M.; Lagutschenkov, A.; Lemaire, J.; Maitre, P.; Boissel, P.; Niedner-Schatteburg, G. *J. Phys. Chem. A* **2004**, *108*, 3350.

JP910035W